Assessment of Refined Higher-Order Shear Deformation Theories for Bending Analysis of Angle-Ply Laminated Sandwich Plates

Madhusudan K. Gollar

Department of Civil Engineering, SDM College of Engineering and Technology, Dharwad, Karnataka, India
Email: *mkgollar123[at]gmail.com*

Abstract: ***Laminated composite and sandwich structures in corporating lightweight flexible cores are widely employed in high-performance aerospace craft, marine hulls, automotive bodies, and civil infrastructure due to their superior specific stiffness, specific strength, and energy absorption characteristics. Accurate flexural modelling of thick sandwich panels requires a precise representation of non-linear transverse shear strain distributions across soft core layers. Conventional First-Order Shear Deformation Theory (FSDT) assumes uniform shear strain through the plate thickness, necessitating artificial shear correction factors and yielding significant errors in thick sandwich configurations. In this investigation, a comprehensive analytical displacement based framework is established utilizing Higher-Order Shear De formation Theories (HSDT) spanning fifth-order (HSDT5) up to thirtieth-order kinematics (HSDT30). Five-layered antisymmetric angle-ply sandwich panels with [15∘/−15∘/core/15∘/−15∘],[30∘/−30∘/core/30∘/−30∘],and [45∘/−45∘/core/45∘/−45∘] stacking sequences under sinusoidal transverse loading are analysed. Naiver analytical closed-form solutions are derived using the Principle of Minimum Potential Energy (PMPE), and transverse shear stresses are evaluated by integrating 3D elasticity equilibrium equations. Extensive parametric studies examine side-to-thickness ratios (a/h = 4 to 100) and core-to-face sheet thickness ratios (tc/tf = 4 to 100). Results demonstrate that FSDT severely underestimates transverse deflections and miscalculates stress fields in thick sandwich panels. Higher order kinematic models satisfy surface traction-free conditions naturally, eliminate shear correction factors, accurately capture bending-twisting coupling, and achieve numerical convergence at HSDT24 and HSDT30.***

Keywords: Higher-Order Shear Deformation Theory, Laminated Sandwich Plates, Angle-Ply Laminates, Stress Analysis, Naiver Solution, Transverse Shear Deformation, MATLAB

1. Introduction

Laminated composite and sandwich structural members are increasingly replacing traditional metallic alloys in weight critical applications including aircraft fuselages, primary satel lite structures, naval hulls, high-speed railway coaches, and wind turbine blades [1], [2]. Laminated composite panels comprise orthotropic fibre-reinforced polymer plies stacked in specified fibre orientations. Composite sandwich panels extend this concept by separating two stiff, high-strength composite face sheets with a low-density core material such as polymeric foam, balsa wood, or metallic honeycomb [3]. This structural configuration maximizes flexural rigidity and moment capacity while maintaining low total mass.

The safe design of advanced composite sandwich components necessitates accurate analytical models capable of predicting flexural deflections, in-plane stresses, and three- dimensional interlaminar shear distributions under operational static and dynamic loads. Classical Plate Theory (CPT), developed on the Kirchhoff-Love hypothesis, assumes that normal planes remain straight and perpendicular to the neutral axis post-deformation. Consequently, CPT neglects transverse shear deformation entirely, restricting its applicability to thin plates ($a/h \geq 100$). First-Order Shear Deformation Theory (FSDT), based on Mindlin-Reissner kinematics, accounts for gross transverse shear distortion by permitting constant shear strain across the plate thickness. However, FSDT fails to represent non-linear shear strain distributions across soft core materials, requires empirical shear correction factors ($ks = 5/6$) to adjust strain energy states, and violates traction-free boundary conditions at upper and lower plate surfaces [4], [5]. Refined Higher-Order Shear Deformation Theories (HSDT) overcome these fundamental drawbacks by expanding the displacement field in higher-order polynomial terms of the thickness coordinate (z). These formulations capture parabolic or higher-degree non-linear transverse shear strain variations through individual layers, satisfy tangential stress continuity across interfaces naturally, and eliminate reliance on subjective shear correction factors [6], [7]. Furthermore, refined displacement fields allow precise evaluation of interlaminar normal and transverse shear stresses, which are critical for predicting failure modes such as face-core delamination, core crimping, and skin wrinkling [8].
The primary objective of this paper is to evaluate a hierarchy of refined higher-order displacement models- ranging from FSDT (5 DOF) up to HSDT30 (30 DOF)- for the bending analysis of five-layered antisymmetric angle-ply laminated sandwich plates. The scope includes:

1) Formulating analytical kinematic displacement field Models incorporating up to thirtieth-order Taylor series Terms for sandwich plates
2) Deriving governing differential equations via the Principle of Minimum Potential Energy and obtaining exact Naiver closed-form solutions for simply supported
3) Computing in-plane normal stresses, in-plane shear Stresses, and transverse shear stresses using both

constitutive equations and 3D elasticity equilibrium integration

4) Performing parametric assessments over varying side to-thickness ratios (a/h), core-to-face thickness ratios (t_c/t_f), and ply orientation angles (15◦, 30◦, 45◦) to establish numerical convergence and evaluate engineering implications

2. Literature Review

Analytical modelling of multi-layered composite and sandwich plates has witnessed substantial development over past decades. Classical theories developed by Kirchhoff and Love provided early foundations for thin isotropic plates but proved incapable of capturing transverse shear deformation in laminated composites. Mindlin and Reissner introduced first-order shear deformation concepts incorporating constant transverse shear strain through the plate thickness. However, the necessity of shear correction factors led researchers to formulate higher order theories.

Swami Nathan and Patil [1] presented a higher-order re fined shear deformation model for static flexure of simply supported sandwich panels, demonstrating that higher-order kinematics eliminate shear rectification factors and provide close agreement with 3D elasticity solutions, particularly for thick core laminates. Tessler et al. [2] developed a Refined Zigzag Theory (RZT) combining coarse FSDT fields with fine zigzag functions, circumventing boundary shear stress constraints and preventing non-physical solution behaviour near plate edges.

Rohwer [3] conducted a comprehensive comparative as assessment of seven plate theories against exact 3D elasticity solutions, establishing that CPT produces unacceptable errors in thick plates due to ignored transverse shear strains. Mantari et al. [4] introduced a higher-order shear deformation theory incorporating trigonometric and exponential functions, satisfying surface traction-free conditions without shear correction factors and delivering accurate stress distributions in thick sandwich panels.

Ye et al. [5] analyzed the flexural and vibration response of sandwich plates with functionally graded soft cores using refined higher-order models derived directly from differential equilibrium equations. Carrera and Ciuffreda [6] formulated the Carrera Unified Formulation (CUF) to systematically eval uate nearly forty plate theories using the Principle of Virtual Displacements (PVD) and Reissner's Mixed Variational The orem (RMVT).

Nguyen et al. [7] developed a refined hyperbolic shear deformation theory employing four displacement variables for bending, buckling, and free vibration of FGM sandwich plates. Zenkour and El-Mekawy [8] investigated inhomogeneous sandwich plates with viscoelastic cores under static loads using sinusoidal shear theories. Natarajan and Ganapati [9] utilized slope discontinuity zigzag functions at face-core interfaces to capture severe transverse shear gradient variations. Zenkour [10] established benchmark analytical Navier solutions for functionally graded sandwich plates under sinusoidal transverse pressure.

Despite these significant contributions, a systematic comparative evaluation spanning high-degree Taylor series displacement formulations up to thirtieth-order kinematics (HSDT30) for soft-core, antisymmetric angle-ply sandwich plates has not been fully documented. This work fills this gap by examining displacement and stress field predictions across a broad spectrum of geometric and lamination parameters.

3. Problem Formulation

Consider a rectangular five-layered antisymmetric angle-ply sandwich plate of length a,width b, and overall thickness h. The panel consists of two composite face sheets, each of thicknesst_f, bonded to a soft lightweight core of thicknesst_c, such that total thickness h = $2t_f$ +t_c. The origin of the Cartesian coordinate system (x, y, z) is positioned at the geometric mid-plane $(z = 0)$, bounded by$-h/2 \leq z \leq h/2$.

The face sheets feature an antisymmetric angle-ply stacking sequence $[\theta/-\theta/\text{core}/\theta/-\theta]$, with fiber orientation angles $\theta \in \{15°, 30°, 45°\}$. The orthotropic material properties for composite face layers (Material 1) are defined as:

$$E_1 = 40\ \text{GPa}, \quad E_2 = 1\ \text{GPa}, \quad E_3 = 1\ \text{GPa},$$
$$G_{12} = 0.5\ \text{GPa}, \quad G_{23} = 0.6\ \text{GPa}, \quad G_{13} = 0.6\ \text{GPa}, \quad \textbf{(1)}$$
$$\nu_{12} = \nu_{13} = \nu_{23} = 0.25$$

The plate is simply supported on all four boundaries (S) and subjected to a sinusoidal transverse pressure load $p_z^+(x, y)$ applied at the upper surface $(z = h/2)$:

$$p_z^+(x, y) = q_0 \sin\left(\frac{\pi x}{a}\right) \sin\left(\frac{\pi y}{b}\right) \quad \textbf{(2)}$$

Where q_0 represents the peak load intensity.

The displacement field is assumed by expanding displacement components$u(x, y, z)$, $v(x, y, z)$, and $w(x, y, z)$ in Taylor series about the mid-plane:

$$u(x, y, z) = u_0(x, y) + z\left(\frac{\partial u}{\partial z}\right)_0 + \frac{z^2}{2!}\left(\frac{\partial^2 u}{\partial z^2}\right)_0 + \frac{z^3}{3!}\left(\frac{\partial^3 u}{\partial z^3}\right)_0 + \cdots$$
$$v(x, y, z) = v_0(x, y) + z\left(\frac{\partial v}{\partial z}\right)_0 + \frac{z^2}{2!}\left(\frac{\partial^2 v}{\partial z^2}\right)_0 + \frac{z^3}{3!}\left(\frac{\partial^3 v}{\partial z^3}\right)_0 + \cdots \quad \textbf{(3)}$$
$$w(x, y, z) = w_0(x, y) + z\left(\frac{\partial w}{\partial z}\right)_0 + \frac{z^2}{2!}\left(\frac{\partial^2 w}{\partial z^2}\right)_0 + \frac{z^3}{3!}\left(\frac{\partial^3 w}{\partial z^3}\right)_0 + \cdots$$

By retaining higher-order terms in the expansion, distinct kinematic theories are defined, separating membrane and flexural response characteristics.

4. Mathematical Formulation

The displacement fields for the evaluated plate theories are defined explicitly below.

a) First-Order Shear Deformation Theory (FSDT)

The FSDT displacement field (Whitney and Pagano) involves 5 primary degrees of freedom:

$u(x,y,z) = u_0 + z\theta_x, v(x,y,z) = v_0 + z\theta_y, w(x,y,z) = w_0$ **(4)**

Where u_0, v_0, w_0 are mid-plane displacements, and θ_x, θ_y are rotations of the normal about the y and x axes.

b) Higher-Order Shear Deformation Theory (HSDT5)

HSDT5 (Pandya and Kant) uses 5 displacement variables with cubic thickness terms that satisfy zero transverse shear stress conditions at $z = \pm h/2$:

$$u = u_0 + z\left[\theta_x - \frac{4}{3}\left(\frac{z}{h}\right)^2\left(\theta_x + \frac{\partial w_0}{\partial x}\right)\right]$$
$$v = v_0 + z\left[\theta_y - \frac{4}{3}\left(\frac{z}{h}\right)^2\left(\theta_y + \frac{\partial w_0}{\partial y}\right)\right], \quad w = w_0 \tag{5}$$

c) Higher-Order Shear Deformation Theory (HSDT12)

HSDT12 (Kant and Manjunatha) incorporates 12 displacement degrees of freedom:

$$\begin{aligned} u &= u_0 + z\theta_x + z^2u_0^* + z^3\theta_x^* \\ v &= v_0 + z\theta_y + z^2v_0^* + z^3\theta_y^* \\ w &= w_0 + z\theta_z + z^2w_0^* + z^3\theta_z^* \end{aligned} \tag{6}$$

d) Refined Higher-Order Theories (HSDT18, HSDT24, HSDT30)

HSDT18 (Rohwer et al.) includes terms up to z^5 (18 DOF). HSDT24 and HSDT30 extend displacement kinematics up to 24 and 30 displacement variables respectively, retaining higher-order powers up to z^7 and z^9:

$$\begin{aligned} u_{\text{HSDT30}} &= u_0 + z\theta_x + z^2u_0^* + z^3\theta_x^* + z^4u_0^{**} + z^5\theta_x^{**} \\ &\quad + z^6u_0^{***} + z^7\theta_x^{***} + z^8u_0^{****} + z^9\theta_x^{****} \\ v_{\text{HSDT30}} &= v_0 + z\theta_y + z^2v_0^* + z^3\theta_y^* + z^4v_0^{**} + z^5\theta_y^{**} \\ &\quad + z^6v_0^{***} + z^7\theta_y^{***} + z^8v_0^{****} + z^9\theta_y^{****} \\ w_{\text{HSDT30}} &= w_0 + z\theta_z + z^2w_0^* + z^3\theta_z^* + z^4w_0^{**} + z^5\theta_z^{**} \\ &\quad + z^6w_0^{***} + z^7\theta_z^{***} + z^8w_0^{****} + z^9\theta_z^{****} \end{aligned} \tag{7}$$

e) Strain-Displacement and Constitutive Equations

Linear strain components in layer (k) are obtained from linear elasticity:

$$\epsilon_x = \frac{\partial u}{\partial x}, \quad \epsilon_y = \frac{\partial v}{\partial y}, \quad \gamma_{xy} = \frac{\partial u}{\partial y} + \frac{\partial v}{\partial x} \tag{8}$$

$$\gamma_{xz} = \frac{\partial u}{\partial z} + \frac{\partial w}{\partial x}, \quad \gamma_{yz} = \frac{\partial v}{\partial z} + \frac{\partial w}{\partial y}, \quad \epsilon_z = \frac{\partial w}{\partial z} \tag{9}$$

The transformed stress-strain relations for an angle-ply layer oriented at angle θ relative to structural axes are:

$$\begin{bmatrix}\sigma_x\\ \sigma_y\\ \tau_{xy}\end{bmatrix}^{(k)} = \begin{bmatrix}\bar{Q}_{11} & \bar{Q}_{12} & \bar{Q}_{16}\\ \bar{Q}_{12} & \bar{Q}_{22} & \bar{Q}_{26}\\ \bar{Q}_{16} & \bar{Q}_{26} & \bar{Q}_{66}\end{bmatrix}^{(k)} \begin{bmatrix}\epsilon_x\\ \epsilon_y\\ \gamma_{xy}\end{bmatrix} \tag{10}$$

where transformed lamina stiffness coefficients $\bar{Q}_{ij}$ are computed from principal elastic moduli using angle transformation relations:

$$\begin{aligned} \bar{Q}_{11} &= Q_{11}m^4 + 2(Q_{12} + 2Q_{66})m^2n^2 + Q_{22}n^4 \\ \bar{Q}_{12} &= (Q_{11} + Q_{22} - 4Q_{66})m^2n^2 + Q_{12}(m^4 + n^4) \\ \bar{Q}_{22} &= Q_{11}n^4 + 2(Q_{12} + 2Q_{66})m^2n^2 + Q_{22}m^4 \quad \mathbf{(11)} \\ \bar{Q}_{16} &= (Q_{11} - Q_{12} - 2Q_{66})m^3n + (Q_{12} - Q_{22} + 2Q_{66})mn^3 \\ \bar{Q}_{26} &= (Q_{11} - Q_{12} - 2Q_{66})mn^3 + (Q_{12} - Q_{22} + 2Q_{66})m^3n \\ \bar{Q}_{66} &= (Q_{11} + Q_{22} - 2Q_{12} - 2Q_{66})m^2n^2 + Q_{66}(m^4 + n^4) \end{aligned}$$

with $m = \cos\theta$ and $n = \sin\theta$.

Transverse shear constitutive relations are given by:

$$\begin{bmatrix}\tau_{yz}\\ \tau_{xz}\end{bmatrix}^{(k)} = \begin{bmatrix}\bar{Q}_{44} & \bar{Q}_{45}\\ \bar{Q}_{45} & \bar{Q}_{55}\end{bmatrix}^{(k)} \begin{bmatrix}\gamma_{yz}\\ \gamma_{xz}\end{bmatrix} \tag{12}$$

where $\bar{Q}_{44} = Q_{44}m^2 + Q_{55}n^2$, $\bar{Q}_{55} = Q_{44}n^2 + Q_{55}m^2$, and $\bar{Q}_{45} = (Q_{55} - Q_{44})mn$

f) Principle of Minimum Potential Energy

Governing equations are derived enforcing variation of total potential energy:

$$\delta\Pi = \delta U - \delta W = 0 \tag{13}$$

where δU is internal strain energy variation, and δW is work done by surface traction p_z^+.

g) Transverse Stresses via 3D Equilibrium Integration

To ensure interlaminar stress continuity, transverse shear stresses τ_{xz}, τ_{yz} are calculated by integrating 3D elasticity equilibrium equation across layer L:

$$\tau_{xz}^{(L)}(z) = -\int_{z_1}^{z}\left(\frac{\partial\sigma_x^{(L)}}{\partial x} + \frac{\partial\tau_{xy}^{(L)}}{\partial y}\right)dz + C_1^{(L)} \tag{14}$$

$$\tau_{yz}^{(L)}(z) = -\int_{z_1}^{z}\left(\frac{\partial\tau_{xy}^{(L)}}{\partial x} + \frac{\partial\sigma_y^{(L)}}{\partial y}\right)dz + C_2^{(L)} \tag{15}$$

Integration constants $C_1^{(L)}, C_2^{(L)}$ are determined using interface stress continuity and traction-free boundary conditions at $z = \pm h/2$.

5. Solution Procedure

a) Navier Double Fourier series Solution

For simply supported edges (S), displacement variables are expanded in double Fourier series. For antisymmetric angle-ply plates, the boundary conditions are satisfied by:

$$\begin{aligned} u_0(x,y) &= \sum_{m=1}^{\infty}\sum_{n=1}^{\infty} u_{0mn}\sin(\alpha x)\cos(\beta y) \\ v_0(x,y) &= \sum_{m=1}^{\infty}\sum_{n=1}^{\infty} v_{0mn}\cos(\alpha x)\sin(\beta y) \quad \mathbf{(16)} \\ w_0(x,y) &= \sum_{m=1}^{\infty}\sum_{n=1}^{\infty} w_{0mn}\sin(\alpha x)\sin(\beta y) \end{aligned}$$

Where $\alpha = m\pi/a$ and$\beta = n\pi/b$.

Substituting Fourier expansions into governing differential equations yields an algebraic system:

$$[K]\{X\} = \{F\} \tag{17}$$

where $[K]$ is the structural stiffness matrix, $\{X\}$ is the vector of Fourier coefficients, and $\{F\}$ is the load vector.

b) Non-Dimensionalization Parameters

Computed output variables are non-dimensionalized as follows:

$$\bar{w} = w\left(\frac{100h^3E_z}{q_0a^4}\right), \quad \bar{\sigma}_x = \sigma_x\left(\frac{h^2}{q_0a^2}\right), \quad \bar{\sigma}_y = \sigma_y\left(\frac{h^2}{q_0a^2}\right)$$

$$\bar{\tau}_{xy} = \tau_{xy}\left(\frac{h^2}{q_0a^2}\right), \quad \bar{\tau}_{xz} = \tau_{xz}\left(\frac{h}{q_0a}\right), \quad \bar{\tau}_{yz} = \tau_{yz}\left(\frac{h}{q_0a}\right)$$

(18)

Evaluation coordinates: $\bar{w}$ at $(a/2, b/2, 0)$; $\bar{\sigma}_x, \bar{\sigma}_y$ at $(a/2, b2, 0)$; $\bar{\tau}_{xy}$ at $(0,0,\pm h/2)$; $\bar{\tau}_{xz}$ at $(0, b/2, 0)$; $\bar{\tau}_{yz}$ at $(a/2, 0, 0)$.

6. Results and Discussion

Parametric studies were conducted for square sandwich plates ($a = b$) across side-to-thickness ratios ($a/h = 4,10,20,50,100$) and core-to-face thickness ratios ($t_c/t_f = 4,10,20,50,100$). Representative numerical comparisons are consolidated in Tables I, II, and III

a) Influence of Side-to-Thickness Ratio (a/h)

As demonstrated in Tables 1 and 2, the side-to-thickness ratio a/h exerts a profound impact on transverse displacement $\bar{w}$ and internal stresses. For thick plates ($a/h = 4$), transverse shear deformation dominates total flexural response. FSDT predicts $\bar{w} = 3.0724$ for $[15°/-15°/\text{core}/15°/-15°]$, whereas HSDT24 and HSDT30 yield $\bar{w} = 79.5181$ and $\bar{w} = 79.9206$ respectively. FSDT underpredicts deflection by more than 2500% because its constant shear strain assumption cannot model severe localized shearing within the soft core layer.

As a/h increases to 100 (thin plate regime), transverse shear flexibility effects vanish, and bending stiffness is governed primarily by in-plane skin extension. Consequently, deflection predictions across all theories converge toward lower values ($\bar{w} \approx 0.905$ to 2.059).

b) Influence of Core Thickness (t_c/t_f)

Table III illustrates the flexural sensitivity to core volume fraction variations ($t_c/t_f = 10$ to 100) for thick panels ($a/h = 4$). Expanding the soft core thickness increases total panel shear compliance dramatically. For $[45°/-45°/\text{core}/45°/-45°]$ panels, increasing t_c/t_f from 4 to 100 escalates HSDT30 transverse displacement $\bar{w}$ from 85.7254 to 860.5468. FSDT captures only a fraction of this increase ($\bar{w} =$ 2.4400 to 37.5758), confirming that lower-order theories are fundamentally unsuited for designing thick sandwich panels with soft cores.

Table I: Non-Dimensionalized Displacements and Stresses In Simply Supported Five-Layered Antisymmetric Angle-Ply Square Sandwich Plates ($t_c/t_f = 4$)

Layup	a/h	Theory	$\bar{w}$	$\bar{\sigma}_x$	$\bar{\sigma}_y$	$\bar{\tau}_{xy}$	$\bar{\tau}_{xz}$	$\bar{\tau}_{yz}$
[15° / −15° / core / 15° / −15°]	4	FSDT	3.0724	0.3958	0.1297	-0.1565	0.2498	0.1286
		HSDT5	8.8475	0.7868	0.2408	-0.2788	0.2008	0.1585
		HSDT12	13.5424	1.4153	0.3489	-0.3908	0.1638	0.1421
		HSDT18	56.4149	4.8600	0.9170	-0.9525	0.0688	0.0673
		HSDT24	79.5181	6.8228	1.2409	-1.2840	0.0241	0.0228
		HSDT30	79.9206	6.8962	1.2229	-1.3010	0.0220	0.0206
	100	FSDT	0.9057	0.5261	0.0878	-0.1128	0.2876	0.0908
		HSDT5	0.9177	0.5262	0.0882	-0.1133	0.2873	0.0911
		HSDT12	0.9296	0.5282	0.0889	-0.1142	0.2867	0.0914
		HSDT18	1.2105	0.5321	0.0995	-0.1247	0.2793	0.0976
		HSDT24	1.9718	0.5522	0.1216	-0.1498	0.2630	0.1108
		HSDT30	2.0591	0.5560	0.1241	-0.1523	0.2615	0.1119
[30° / −30° / core / 30° / −30°]	4	FSDT	2.5967	0.2803	0.1510	-0.1948	0.2203	0.1592
		HSDT5	8.1961	0.5580	0.3003	-0.3696	0.1942	0.1692
		HSDT12	13.0280	1.0179	0.5014	-0.5863	0.1625	0.1490
		HSDT18	60.0935	3.5505	1.5737	-1.7089	0.0723	0.0722
		HSDT24	86.2221	5.1121	2.2396	-2.4097	0.0259	0.0253
		HSDT30	86.8409	5.1669	2.2457	-2.4446	0.0238	0.0230
	100	FSDT	0.7140	0.3332	0.1390	-0.1745	0.2345	0.1449
		HSDT5	0.7237	0.3334	0.1393	-0.1749	0.2344	0.1450
		HSDT12	0.7330	0.3347	0.1401	-0.1761	0.2341	0.1451
		HSDT18	0.9666	0.3407	0.1476	-0.1848	0.2313	0.1470
		HSDT24	1.6382	0.3614	0.1660	-0.2085	0.2247	0.1511
		HSDT30	1.7195	0.3650	0.1687	-0.2112	0.2241	0.1515
[45° / −45° / core / 45° / −45°]	4	FSDT	2.4400	0.2113	0.2113	-0.1973	0.1898	0.1898
		HSDT5	7.9472	0.4240	0.4240	-0.3911	0.1819	0.1819
		HSDT12	12.7622	0.7316	0.7316	-0.6702	0.1557	0.1557
		HSDT18	59.5816	2.3353	2.3353	-2.1351	0.0716	0.0716
		HSDT24	85.0786	3.3318	3.3318	-3.0302	0.0252	0.0252
		HSDT30	85.7254	3.3603	3.3603	-3.0737	0.0231	0.0231
	100	FSDT	0.6454	0.2113	0.2113	-0.1973	0.1898	0.1898

Layup	a/h	Theory	$\bar{w}$	$\bar{\sigma}_x$	$\bar{\sigma}_y$	$\bar{\tau}_{xy}$	$\bar{\tau}_{xz}$	$\bar{\tau}_{yz}$
		HSDT5	0.6545	0.2117	0.2117	-0.1976	0.1898	0.1898
		HSDT12	0.6631	0.2125	0.2125	-0.1992	0.1897	0.1897
		HSDT18	0.8834	0.2207	0.2207	-0.2063	0.1893	0.1893
		HSDT24	1.5285	0.2433	0.2433	-0.2280	0.1881	0.1881
		HSDT30	1.6082	0.2467	0.2467	-0.2307	0.1879	0.1879

c) Ply Orientation and Bending-Twisting coupling

The ply orientation angle θ introduces distinct anisotropic behavior:

1) **Asymmetric Stress Distribution ($15°, 30°$)**: For 15° and 30° angle-ply layups, $\bar{\sigma}_x > \bar{\sigma}_y$ because stiffer fiber axes align closer to the x-direction. In Table 1 ($a/h = 4$, HSDT30), 15° lamination yields $\bar{\sigma}_x = 6.8962$ versus $\bar{\sigma}_y = 1.2229$.
2) **Symmetric Stress State** (45°): For $[45°/-45°/\text{core}/45°/-45°]$, equal ply orientation relative to global orthogonal axes produces identical normal stresses ($\bar{\sigma}_x = \bar{\sigma}_y$) and identical transverse shear stresses ($\bar{\tau}_{xz} = \bar{\tau}_{yz}$) across all theories and geometric ratios.
3) **Bending-Twisting Coupling**: The twisting shear stress $\bar{\tau}_{xy}$ remains negative across all cases, directly reflecting bending-twisting coupling in antisymmetric angle-ply stacking. Refined theories (HSDT24/30) capture higher twisting stress magnitudes, proving their enhanced fidelity in modelling coupled extension-flexure-twist modes.

Table II: Non-Dimensionalized Displacements and Stresses for Intermediate Slenderness Ratio ($a/h = 20$, $t_c/t_f = 4$)

Layup	a/h	Theory	$\bar{w}$	$\bar{\sigma}_x$	$\bar{\sigma}_y$	$\bar{\tau}_{xy}$	$\bar{\tau}_{xz}$	$\bar{\tau}_{yz}$
[15° / −15°]	20	FSDT	0.9964	0.5185	0.0902	-0.1153	0.2854	0.0930
		HSDT5	1.2881	0.5225	0.1004	-0.1264	0.2780	0.0995
		HSDT12	1.5854	0.5435	0.1098	-0.1392	0.2696	0.1045
		HSDT18	7.0975	0.8530	0.2458	-0.2664	0.2035	0.1474
		HSDT24	19.2697	1.8065	0.4046	-0.4526	0.1599	0.1417
		HSDT30	20.5339	1.9125	0.4202	-0.4704	0.1572	0.1392
[30° / −30°]	20	FSDT	0.7876	0.3303	0.1396	-0.1755	0.2338	0.1457
		HSDT5	1.0298	0.3368	0.1472	-0.1851	0.2310	0.1478
		HSDT12	1.2832	0.3525	0.1567	-0.1992	0.2270	0.1488
		HSDT18	6.5601	0.5845	0.3086	-0.3574	0.1937	0.1623
		HSDT24	19.1561	1.2623	0.6000	-0.6931	0.1604	0.1493
		HSDT30	20.4878	1.3404	0.6332	-0.7280	0.1578	0.1469
[45° / −45°]	20	FSDT	0.7144	0.2113	0.2113	-0.1973	0.1898	0.1898
		HSDT5	0.9423	0.2201	0.2201	-0.2053	0.1895	0.1895
		HSDT12	1.1824	0.2330	0.2330	-0.2197	0.1880	0.1880
		HSDT18	6.3455	0.4278	0.4278	-0.3870	0.1782	0.1782
		HSDT24	18.9155	0.8754	0.8754	-0.8106	0.1547	0.1547
		HSDT30	20.2456	0.9269	0.9269	-0.8562	0.1522	0.1522

Table III: Effect of Core-to-Face Thickness Ratio (t_c/t_f) on Non-Dimensionalized Response of Thick Sandwich Plates ($a/h = 4$)

Layup	t_c/t_f	Theory	$\bar{w}$	$\bar{\sigma}_x$	$\bar{\sigma}_y$	$\bar{\tau}_{xy}$	$\bar{\tau}_{xz}$	$\bar{\tau}_{yz}$
[15° / −15° / core / 15° / −15°]	10	FSDT	5.7865	0.6437	0.2256	-0.2752	0.2246	0.1220
		HSDT5	46.3577	1.9863	0.5800	-0.6595	0.1672	0.1633
		HSDT12	96.6379	4.7793	1.1451	-1.1413	0.1434	0.1465
		HSDT18	345.2423	15.0290	2.6396	-2.9444	0.0879	0.0866
		HSDT24	338.0118	15.4243	3.0265	-2.9724	0.0870	0.0856
		HSDT30	365.8803	16.5789	3.0392	-3.2027	0.0812	0.0801
	100	FSDT	46.1642	4.6195	1.6930	-2.0864	0.2055	0.1165
		HSDT5	793.2401	6.5210	3.0471	-3.5460	0.1602	0.1526
		HSDT12	804.9053	6.9728	3.3421	-3.4552	0.1591	0.1515
		HSDT18	839.0909	6.5323	2.1704	-3.6153	0.1616	0.1548
		HSDT24	845.8370	6.1192	1.5996	-3.6154	0.1620	0.1550
		HSDT30	873.9949	6.6991	2.2794	-3.6286	0.1621	0.1552
[45° / −45° / core / 45° / −45°]	10	FSDT	4.6564	0.3619	0.3619	-0.3387	0.1734	0.1734
		HSDT5	44.6729	1.0810	1.0810	-0.9911	0.1663	0.1663
		HSDT12	95.9273	2.4621	2.4621	-2.1651	0.1466	0.1466
		HSDT18	358.7500	7.0411	7.0411	-6.5664	0.0908	0.0908
		HSDT24	351.2171	7.4304	7.4304	-6.6313	0.0899	0.0899
		HSDT30	381.5872	7.8942	7.8942	-7.2098	0.0843	0.0843
	100	FSDT	37.5758	2.7062	2.7062	-2.5368	0.1609	0.1609

Layup	t_c/t_f	Theory	$\bar{w}$	$\bar{\sigma}_x$	$\bar{\sigma}_y$	$\bar{\tau}_{xy}$	$\bar{\tau}_{xz}$	$\bar{\tau}_{yz}$
		HSDT5	779.1453	4.4772	4.4772	-4.1412	0.1562	0.1562
		HSDT12	791.2022	4.8036	4.8036	-4.1696	0.1551	0.1551
		HSDT18	825.6297	3.9567	3.9567	-4.4052	0.1580	0.1580
		HSDT24	832.3548	3.4525	3.4525	-4.3873	0.1583	0.1583
		HSDT30	860.5468	4.0532	4.0532	-4.4324	0.1585	0.1585

d) Through Thickness Stress Profiles and Convergence

Computing transverse shear stresses $\bar{\tau}_{xz}$ and $\bar{\tau}_{yz}$ by integrating 3D elasticity equilibrium equations ensures continuous interlaminar shear stress profiles across face-core interfaces while naturally satisfying parabolic traction-free surface conditions at $z = \pm h/2$. Numerical results for HSDT24 and HSDT30 exhibit minor variance across all cases, confirming complete numerical convergence at higher-order Taylor series displacement expansions.

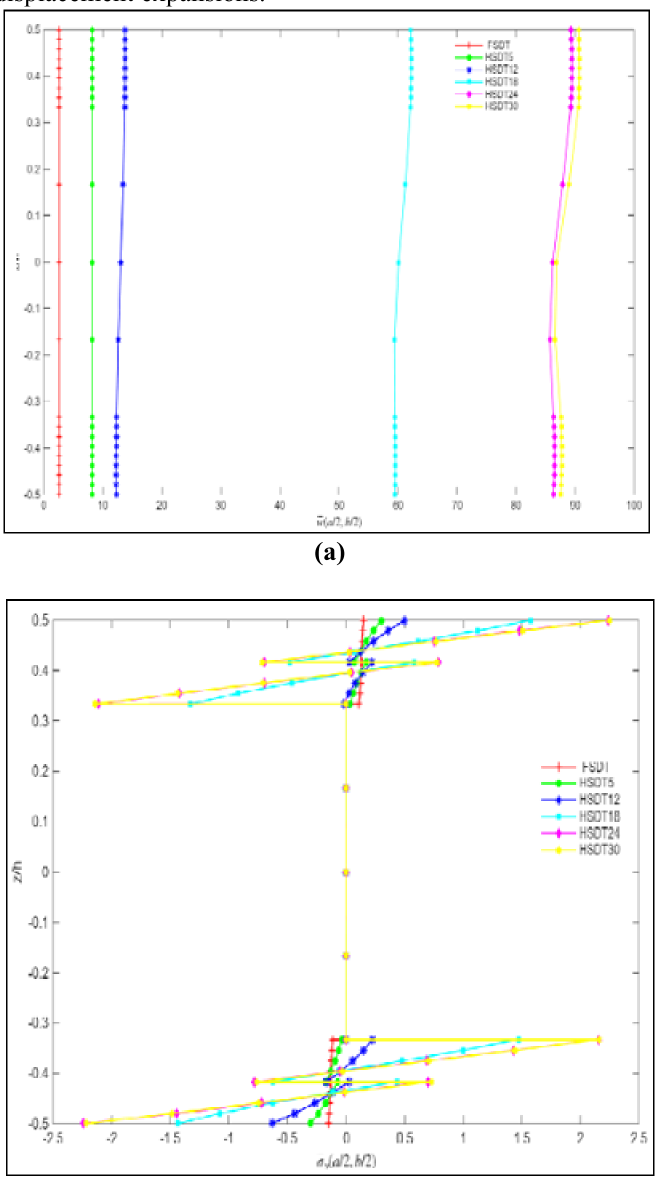

(a)

(b)

Figure 1: Through-thickness response profiles across different shear deformation theories: (a) non-dimensionalized transverse deflection$\bar{w}(a/2, b/2)$, and (b) non-dimensionalized normal stress$\bar{\sigma}_y(a/2, b/2)$.

7. Conclusion

This study presented a detailed comparative evaluation of refined higher-order shear deformation theories (FSDT through HSDT30) for bending analysis of simply supported antisymmetric angle-ply laminated sandwich plates subjected to sinusoidal transverse loading. Navier analytical closed-form solutions derived via the Principle of Minimum Potential Energy demonstrated that First-Order Shear Deformation Theory (FSDT) is fundamentally inadequate for thick soft-core sandwich panels, severely underestimating deflections and miscalculating stress distributions.

Refined higher-order theories naturally satisfy traction-free surface conditions, eliminate empirical shear correction factors, and accurately capture non-linear shear warping through flexible cores. Stacking at 45° angle-ply produces perfectly symmetric normal ($\bar{\sigma}_x = \bar{\sigma}_y$) and transverse shear ($\bar{\tau}_{xz} = \bar{\tau}_{yz}$) stress fields. Kinematic formulations achieve numerical convergence at HSDT24 and HSDT30, establishing reliable benchmark tools for advanced aerospace, marine, and civil composite design. As illustrated in Fig. 1(a) and (b), the through-thickness profiles clearly depict the accuracy and convergence of higher-order kinematic models compared to FSDT

Acknowledgment

The authors gratefully acknowledge the guidance and academic support provided by Dr. R. J. Fernandes, Head of Civil Engineering, SDM College of Engineering and Technology, Dharwad, India.

References

[1] K. Swami Nathan and S. S. Patil, "Analytical evaluation of higher order refined computational models," *Composite Structures*, vol. 75, pp. 114–120, 2006.

[2] A. Tessler, M. Di Sciuva, and M. Gherlone, "Refined Zigzag Theory for Homogeneous, Laminated Composite, and Sandwich Plates," NASA Technical Publication NASA/TP-2010-216214, 2010

[3] K. Rohwer, "Application of Higher Order Theories to the Bending Analysis of Layered Composite Plates," *Int. J. Solids Struct.*, vol. 28, no. 1, pp. 105–119, 1990.

[4] J. L. Mantari, A. S. Oktem, and C. Guedes Soares, "A new higher order shear deformation theory for sandwich and composite laminated plates," *Compos. Part B Eng.*, vol. 43, pp. 1489–1499, 2012.

[5] R. Ye, N. Zhao, D. Yang, J. Cui, O. Gaidai, and P. Ren, "Bending and free vibration analysis of sandwich plates

with functionally graded soft core," *J. Sandw. Struct. Mater.*, vol. 22, no. 8, pp. 1–31, 2020.

[6] E. Carrera and A. Ciuffreda, "A unified formulation to assess theories of multi-layered plates for various bending problems," *Composite Structures*, vol. 69, pp. 271–293, 2004.

[7] K. T. Nguyen, T. H. Thai, and T. P. Vo, "A Refined Higher-Order Shear Deformation Theory For Bending, Vibration and Buckling Analysis," *Int. J. Mech. Sci.*, vol. 96–97, pp. 46–65, 2015

[8] A. M. Zenkour and H. F. El-Mekawy, "Bending of inhomogeneous sandwich plates with viscoelastic cores," *J. Sandw. Struct. Mater.*, vol. 16, pp. 1416–1438, 2014.

[9] S. Natarajan and Ganapati, "Bending and vibration of functionally graded material sandwich plates using an accurate theory," *Fin. Elem. Anal. Des.*, vol. 57, pp. 32–42, 2012

[10] A. M. Zenkour, "A comprehensive analysis of functionally graded sandwich plates: Part 1—Deflection and stresses," *Int. J. Solids Struct.*, vol. 42, pp. 5224–5242, 2005.